# Vibrational coherence in nonadiabatic dynamics

M. Bixon and Joshua Jortner
*The Raymond and Beverly Sackler Faculty of Exact Sciences, School of Chemistry, Tel Aviv University, Ramat Aviv, Tel Aviv 69978, Israel*

(Received 24 December 1996; accepted 4 April 1997)

In this paper we explore temporal vibrational coherence effects in nonadiabatic radiationless transitions between two electronic states in a large molecule or in the condensed phase, accounting explicitly for the role of the (intramolecular and/or medium) vibrational quasicontinuum of the final states. Our treatment of the time evolution of the wave packet of states and of coherence effects in the nonradiative population probabilities of the reactants and the products rests on the diagonalization of the Hamiltonian of the entire multimode system, with supplementary information being inferred from the effective Hamiltonian formalism. New features of the vibrational Franck–Condon quasicontinuum, which originate from weak, but finite, correlations between off-diagonal coupling terms, were established. The state dependence of the off-diagonal couplings $V_{s\alpha}$ between the doorway states manifold $\{|s\rangle\}$ and the quasicontinuum $\{|\alpha\rangle\}$ was quantified by the correlation parameters $\eta_{ss'}=\langle V_{s\alpha}V_{\alpha s'}\rangle/[\langle V_{s\alpha}^2\rangle\langle V_{s'\alpha}^2\rangle]^{1/2}$, where $\langle\ \rangle$ denotes the average over the relevant energy range. Calculations were conducted for a Franck–Condon four-mode system consisting of $n_s=100$ doorway states and $n_\alpha=3000$ quasicontinuum states. The correlation parameters for all pairs of doorway states are considerably lower than unity ($|\eta_{ss'}|\lesssim 0.4$), obeying propensity rules with the highest values of $|\eta_{ss'}|$ corresponding to a single vibrational quantum difference, while for multimode changes between $|s\rangle$ and $|s'\rangle$ very low values of $|\eta_{ss'}|$ are established. Quantum beats in the population probabilities of products and reactants in nonadiabatic dynamics are characterized by an upper limit for their modulation amplitudes $\xi\cong(\Gamma/\Delta E)\,\eta$ (for $\Delta E/2\pi\Gamma\geqslant 1$), where $\Gamma$ is the decay width of the doorway states and $\Delta E$ is their energetic spacing. These low $\xi$ values originate from a small ($\sim\Gamma/\Delta E$) contribution to the off-diagonal matrix elements of the nonradiative decay matrix in conjunction with low correlation parameters. The amplitudes of the quantum beats in nonradiative temporal dynamics provide dynamic information on the larger correlation parameters $\eta_{ss'}$. Our theoretical and numerical analysis was applied for temporal coherence effects in nonadiabatic electron transfer dynamics in a Franck–Condon quasicontinuum of Mulliken charge transfer complexes [K. Wynne, G. Reid, and R. M. Hochstrasser, J. Chem. Phys. **105**, 2287 (1996)]. This accounts for the ''preparation'' (signature of coherent excitation), for the low amplitudes of coherent temporal modulation of reactants and products ($\xi\cong 0.05-0.06$ determined by the $\eta_{ss'}$ parameters) and for the dominating contributions to temporal coherence (subjected to propensity rules).  [S0021-9606(97)02226-5]

## I. INTRODUCTION

The advent of femtosecond (fs) dynamics on the time scale of nuclear motion[1–3] opened up new horizons in the exploration of ultrafast nonradiative processes. Interstate and intrastate relaxation in isolated large molecules, in clusters, and in the condensed phase is well understood,[1–6] while the interplay between energy relaxation and dephasing[1–31] is actively pursued, being of considerable current interest. Vibrational (or electronic–vibrational) coherence effects in a variety of systems were experimentally explored, ranging from small diatomic molecules[7–11] to huge biophysical systems.[27–31] These vibrational coherence effects originate from the time evolution of wave packets of nuclear states, which are manifested by oscillatory time evolution, i.e., quantum beats, with the characteristic frequencies corresponding to the energy differences between the coherently excited nuclear (or electronic–nuclear) states. The origin of the exploration of molecular quantum beats can be traced to the predictions of the time evolution of coherently excited wave packets of mixed interstate or intrastate manifolds,[32] while the utilization of femtosecond lasers resulted in rich information on vibrational coherence effects.[1–31,33–38] Vibrational coherence effects in clusters and in the condensed phase fall into several categories.

(A) Vibrational coherence in reactant states. The doorway (reactant) states are coherently excited by a broadband fs laser excitation and their time evolution is interrogated by pump–probe[1–3] or by (spontaneous or stimulated) fluorescence.[1–3] In this category, ''small'' subsystems correspond to the dynamics of a diatomic in liquids, fluids, and solids (e.g., $I_2$ in liquid hexane,[26,33] in fluid rare gases,[12] and in solid Ar[18]), or in clusters [e.g., $I_2Ar_N$ (Ref. 13) or $I_2^-(CO_2)_N$ (Refs. 14 and 15)]. Large systems exhibiting quantum beats in their doorway states correspond to the vibrational wave packets in the electronically excited state of the bacteriochlorophyll dimer ($^1P^*$), which constitutes the primary electron donor in the photosynthetic reaction center[27] and vibrational wave packets in the bacteriochloro-

 0021-9606/97/107(5)/1470/13/$10.00 

phyll subcomponents of the bacterial photosynthetic antenna[30,31] for electronic energy transfer

(B) Vibrational coherence in the product states.

(B1) Impact excitation of vibrational wave packets of dissociative products. These involve diatomics produced from fs photodissociaton in solution, e.g., $I_3^- \rightarrow I_2^- + I$,[16] and $HgI_2 \rightarrow HgI + I$.[19] For large systems these involve quantum beats in the vibrationally excited hemoglobin (Hb) produced from fs dissociation of Hb·NO.[28]

(B2) Excitation of vibrational coherence via isomerization. Femtosecond-induced *cis→trans* isomerization of stilbene[20] and of rhodopsin and bacteriorhodopsin[29] results in a vibrational wave packet of the product.

(B3) Excitation of vibrational coherence via nonadiabatic multiphonon processes, e.g., intermolecular electron transfer (ET). Intermolecular ET[34] in Mulliken charge transfer donor $(D)$–acceptor $(A)$ complexes[35] excited by fs laser pulses corresponds to

$$DA \xrightarrow{h\nu} D^+A^- \rightarrow (DA)(v) \tag{1.1}$$

(where $v$ denotes a vibrationally excited ground state). Coherent oscillations were observed by Wynne, Galli, Reid and Hochstrasser in the ground electronic state $(DA)^{(v)}$ absorption bleach signal of hexamethylbenzene-tetracyanoethylene (TCNE)[34(a)] and of pyrene–TCNE[34(b)] complexes. Concurrently, coherent oscillations were also observed in the stimulated emission gain signal of pyrene–TCNE,[34(b)] manifesting vibrational coherence of the reactant doorway vibrational state of $D^+A^-$ [category (A)].

The ubiquity of vibrational coherence effects raises the conceptual question of the distinction between the experimental conditions of preparation and interrogation and the intrinsic aspects of relaxation and dephasing dynamics. The experimental observations of vibrational coherence effects in chemical and biophysical systems triggered theoretical studies,[1–4,21–26,36–38] which rest on the equations of motion of the density matrix,[21,24–26,36,37] on the semigroup formalism,[38] and on the Redfield equations.[22] Such theoretical studies suffer from some intrinsic limitations. The separation of the system and the bath, which is explicit in the Redfield formalism,[39] implicitly implies that the correlation time of the bath is very short, an assumption which may be inapplicable for ultrafast fs dynamics of the system. Furthermore, these theoretical studies[21–26,36–38] focused on the dynamics of small systems, or alternatively separated out a single vibrational mode in a large system. In the context of the fs dynamics of large molecular and condensed phase systems the central role of the (intramolecular and/or medium) vibrational quasicontinuum was not considered. In this paper we explicitly consider the essential role of the vibrational quasicontinuum for coherence effects in a nonradiative transition between two electronic states, e.g., radiationless transitions in an isolated large molecule or nonadiabatic dynamics in the condensed phase. Our treatment is based on the exact diagonalization of the Hamiltonian of the entire multimode system. Supplementary information was inferred from model calculations which rest on the effective Hamiltonian formalism. New features of a realistic vibrational quasicontinuum, which originate from weak but finite correlations between the off-diagonal coupling terms, emerge from our study. In what follows we analyze the dynamic implications of vibrational coherence in reactant states [category (A)] and in product states [category (B3)] in a system undergoing nonadiabatic transition between zero-order vibronic manifolds, which correspond to two different electronic states (Fig. 1), e.g., radiationless transitions in an isolated large molecule or nonadiabatic dynamics in the condensed phase. The theory will be explicitly applied to the interpretation of the experimental results of Hochstrasser *et al.*[34] for the weak temporal modulation (i.e., quantum beats with a frequency of $170\ cm^{-1}$ which corresponds to the perpendicular $D^+A^-$ motion),[34(b)] superimposed on the buildup of product states $(DA)^v$ and on the decay of reactant states $D^+A^-$, Eq. (1.1), in charge transfer complexes.

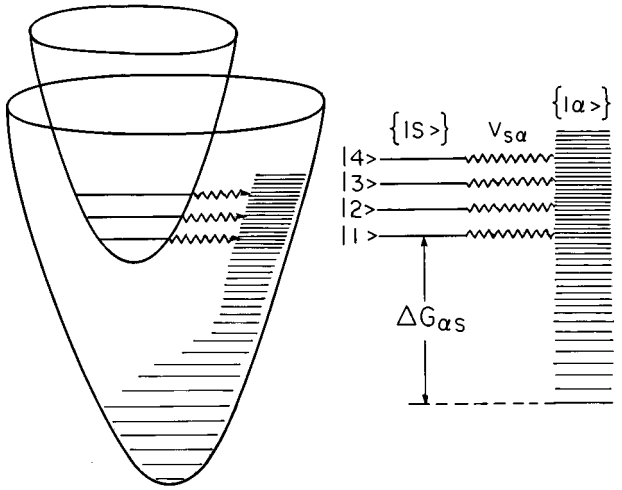


FIG. 1. Energy levels scheme for nonadiabatic dynamics. The vibronic manifold of the doorway states $\{|s\rangle\}$ is coupled to the dissipative quasicontinuum $\{|\alpha\rangle\}$.

## II. COHERENCE IN INTRAMOLECULAR AND CONDENSED PHASE DYNAMICS

The level structure, coupling, and accessibility of the model system considered herein consist of distinct vibronic manifolds of two electronic states (Fig. 1): (i) the doorway states $\{|s\rangle\}$ $(s=1,2,3,\ldots,N)$, which carry oscillator strengths from the (single) ground state $|g\rangle$. (ii) The dissipative quasicontinuum states $\{|\alpha\rangle\}$, which correspond to a lower lying electronic configuration and which do not carry oscillator strengths from $|g\rangle$. The doorway states are coupled to the quasicontinuum via the interstate nonadiabatic couplings $V_{s\alpha}=\langle s|H|\alpha\rangle$ (where $H$ is the system's Hamiltonian). When the dissipative quasicontinuum corresponds to the ground electronic state, the $|g\rangle$ state corrsponds to the lowest-vibronic state (i.e., the zero-point energy) of the $\{|\alpha\rangle\}$ manifold. In the intramolecular dynamics $\{|s\rangle\}$ and $\{|\alpha\rangle\}$ correspond to vibronic manifolds of two electronic states of a large isolated molecule. In nonadiabatic dynamics of a large molecule in a condensed phase $\{|s\rangle\}$ and $\{|\alpha\rangle\}$ represent

intramolecular+medium vibronic states of the initial and final electronic manifolds, with $\{|s\rangle\}$ being the reactant manifold and $\{|\alpha\rangle\}$ corresponding to the product manifold. In the case of ET within a solvated supermolecule, $D^+A^-$ is the $\{|s\rangle\}$ reactant manifold and $DA$ is the $\{|\alpha\rangle\}$ product quasicontinuum. The Hamiltonian of the system is

$$\underset{\approx}{H}=\sum_s |s\rangle E_s\langle s|+\sum_\alpha |\alpha\rangle E_\alpha\langle\alpha|+\sum_s\sum_\alpha |s\rangle \times V_{s\alpha}\langle\alpha|+\text{cc}. \tag{2.1}$$

We consider in Eq. (2.1) the entire system without decomposition into the ''relevant'' system and a ''bath.''

A coherent optical excitation of the system results in a wave packet of (vibrational) doorway states

$$\Psi(0)=\sum_s A_s(0)|s\rangle, \tag{2.2}$$

where the excitation amplitudes $A_s(0)$ are determined by the excitation conditions. A more general treatment of the rise and fall of excited manifold under (weak field) optical excitation can be given, but this does not modify the general features of temporal coherence effects. The time evolution of the wave packet of the states of the entire system is

$$\Psi(t)=\sum_s A_s(t)|s\rangle+\sum_\alpha B_\alpha(t)|\alpha\rangle. \tag{2.3}$$

Using the Hamiltonian, Eq. (2.1), and the coefficients in the interaction representation

$$a_s(t)=\exp(iE_st/\hbar)A_s(t),$$
$$b_\alpha(t)=\exp(iE_\alpha t/\hbar)B_\alpha(t), \tag{2.4}$$

results in the equations of motion for the amplitudes of the doorway states

$$-\hbar^2\dot{a}_s(t)=\int_0^t dt'\sum_\alpha |V_{s\alpha}|^2\exp[-i\omega_{s\alpha}(t-t')]a_s(t') + \int_0^t dt'\sum_\alpha\sum_{s'\neq s} V_{s\alpha}V_{\alpha s'} \times\exp[-i(\omega_{s\alpha}t-\omega_{s'\alpha}t')]a_{s'}(t'), \tag{2.5}$$

where $\omega_{s\alpha}=(E_\alpha-E_s)/\hbar$. Equation (2.5) will be recast in Sec. III for several coupling schemes.

The time evolution and the nature of the coherence effects (quantum beats) is determined by the character of the dynamic observables, i.e., by the experimental interrogation method. These dynamic observables are determined by the amplitudes $\{A_s(t)\}$ of the doorway states in Eq. (2.3). We consider the population probability of the reactant doorway states manifold $\{|s\rangle\}$,

$$P(t)=\sum_s |\langle s|\Psi(t)\rangle|^2=\sum_s |A_s(t)|^2. \tag{2.6}$$

The effective rate is

$$k(t)=d\ \ln P(t)/dt = \left[\sum_s \dot{A}_s^*(t)A_s(t)+\text{cc}\right]\Big/\sum_s |A_s(t)|^2 \tag{2.7}$$

(where the dot denotes the time derivative). The population of the product states is

$$P_\alpha(t)=\sum_\alpha |\langle\alpha|\Psi(t)\rangle|^2=1-P(t). \tag{2.8}$$

Similarly, the photon counting rate for the spontaneous radiative decay to $|g\rangle$, i.e.,

$$I(t)=|\langle g|\hat{\mu}|\Psi(t)\rangle|^2 \tag{2.9a}$$

is given by

$$I(t)=\sum_s |\mu_{\text{gs}}|^2|A_s(t)|^2+\sum_{s\neq s'}\sum \mu_{\text{gs}}\mu^*_{\text{gs}'}A_s(t)A^*_{s'}(t), \tag{2.9b}$$

where $\{\mu_{\text{gs}}\}$ are the transition moments for emission from the doorway states to the ground (final) state, which are proportional to the Franck–Condon vibrational overlap integrals for radiative decay. $I(t)$ consists of a direct $(s=s')$ term, whose structure is similar to $P(t)$, Eq. (2.6), and mixed $(s\neq s')$ terms. Equation (2.9a) implies a single final ground state (gs) and can be readily extended by the summation over a $\{|g\rangle\}$ gs manifold with the $\{\mu_{\text{gs}}\}$ terms in Eq. (2.9b) containing the appropriate vibrational overlaps for the radiative transitions.

The study of temporal dynamic observables requires the amplitude $\{A_s(t)\}$ of the doorway states, Eq. (2.3). For this purpose it will be useful to write the equations of motion in terms of the effective Hamiltonian formalism.[32(b),40] The initial conditions are given by Eq. (2.2). The time evolution of the subsystem of the discrete $\{|s\rangle\}$ manifold of the doorway states is determined by the effective Hamiltonian[40]

$$\underset{\approx}{H}_{\text{eff}}=\underset{\approx}{H}_0-(i/2)\underset{\approx}{\Gamma}, \tag{2.10}$$

where $\underset{\approx}{H}_0$ is the Hamiltonian in the discrete $\{|s\rangle\}$ (Hilbert) subspace

$$(\underset{\approx}{H}_0)_{ss'}=E_s\delta_{ss'} \tag{2.11}$$

and $\underset{\approx}{\Gamma}$ is the decay matrix

$$(\underset{\approx}{\Gamma})_{ss'}=2\pi\langle V_{s\alpha}V_{\alpha s'}\rangle\rho, \tag{2.12}$$

where $\langle\ \rangle$ denotes the average over the relevant energy range $\delta E$, where the density of states is $\rho$, i.e.,

$$\langle V_{s\alpha}V_{\alpha s'}\rangle=\left(\frac{1}{\rho\,\delta E}\right)\sum_{\substack{\alpha\\ E_s,E_{s'}\in\delta E}} V_{s\alpha}V_{\alpha s'}. \tag{2.13}$$

The energy range $\delta E$ includes the energies of the doorway states $E_s$ and $E_{s'}$ and has to span the $E_\alpha$ domain of the relevant $\{|\alpha\rangle\}$ states which contribute to interference between $|s\rangle$ and $|s'\rangle$. It should be noted that if $\delta E\to\infty$ and the sum over the $\{|\alpha\rangle\}$ states includes the entire manifold, then $\langle V_{s\alpha}V_{\alpha s'}\rangle=0(s\neq s')$. The energy range $\delta E$ has to be taken as finite, to include the subset of the relevant $\{|\alpha\rangle\}$ states, i.e.,

$\delta E \gtrsim |E_s - E_{s'}|$. We shall take $\delta E = d|E_s - E_{s'}|$, where $d \cong 5$. Numerical calculations show that the averaged product $\langle V_{s\alpha} V_{\alpha s'} \rangle$ taken over the energy range $\delta E$ is not sensitive to the magnitude of the parameter $d$ specified above.

Temporal coherence effects manifested in the modulation of the nonradiative transition probability will be exhibited when the following conditions are satisfied: (1) A coherent wave packet, Eq. (2.3), is initially prepared. (2) The doorway states decay into a common channel (i.e., a vibronic quasicontinuum or a radiative continuum[40]). (3) The off-diagonal terms of the decay matrix, Eqs. (2.12) and (2.13), are nonvanishing. The equations of motion for the amplitudes $\{A_s(t)\}$, Eq. (2.3), in the discrete Hilbert subspace are:

$$\left(\frac{\hbar}{i}\right) \frac{d}{dt} \underset{\sim}{A}_s(t) = \underset{\approx}{H}_{\rm eff} \underset{\sim}{A}_s(t), \tag{2.14}$$

where $\underset{\sim}{A}_s(t)$ is the vector of the coefficient $\{A_s(t)\}$ in Eq. (2.3). The effective Hamiltonian, Eq. (2.4), is diagonalized by the transformation

$$\underset{\approx}{D} \underset{\approx}{H}_{\rm eff} \underset{\approx}{D}^{-1} = \underset{\approx}{\Lambda}, \tag{2.15}$$

where $\underset{\approx}{\Lambda}$ is diagonal, resulting in the time evolution

$$\underset{\sim}{A}_s(t) = \underset{\approx}{D}^{-1} \exp\left(\frac{-i}{\hbar} \underset{\approx}{\Lambda} t\right) \underset{\approx}{D} \underset{\sim}{A}_s(0). \tag{2.16}$$

We now turn to the coherence effects in the dynamic observables, i.e., the nonradiative population probabilities of reactants $P(t)$, Eq. (2.6), of products $P_\alpha(t)$, Eq. (2.8), and the photon counting rate $I(t)$, Eq. (2.9). From the preceding analysis we note that radiative decay interference effects of a coherently excited wave packet are always exhibited in the photon counting rate $I(t)$, due to the second ''mixed'' ($s \neq s'$) terms on the right-hand side (rhs) of Eq. (2.9). This is the well-known case of decay of ''distinguishable levels'' into the common radiative continuum.[32(b)] For the population probabilities of the reactant (doorway states $\{|s\rangle\}$) or product (quasicontinuum states $\{|\alpha\rangle\}$) manifolds, the population probabilities, Eqs. (2.6) and (2.8), contain only the ''direct'' ($s = s'$) terms. It is apparent from Eqs. (2.15) and (2.16) that a necessary condition for the appearance of coherent effects in the nonradiative decay is the existence of a nondiagonal decay matrix, Eqs. (2.12) and (2.13). We shall address the explicit characterization of interference effects in the decay to a dissipative vibronic quasicontinuum, as manifested by the off-diagonal elements of the decay matrix. The magnitude of these off-diagonal matrix elements of $\underset{\approx}{\Gamma}$ pertains to the correlation between the coupling matrix elements, i.e., $V_{s\alpha}$, $V_{s'\alpha}$ ($s \neq s'$), which will now be considered.

## III. CORRELATIONS IN INTERSTATE COUPLING

The exploration of temporal coherence effects requires explicit expressions for the decay matrix $\underset{\approx}{\Gamma}$, Eq. (2.12). For this purpose we shall make contact between the equations of motion, Eqs. (2.5) and (2.4), for the doorway amplitudes $\{A_s(t)\}$ and the equations of motion within the framework of the effective Hamiltonian formalism, Eq. (2.14). This connection will be established for several coupling schemes.

### A. The constant-coupling approximation

In this scheme[41] the coupling terms $V_{s\alpha}$ are independent of the specific final state $\alpha$. Furthermore, we assume that the final states $\{|\alpha\rangle\}$ are homogeneously distributed with a constant near-neighbor distance $\epsilon = \rho^{-1}$ (where $\rho$ is the density of states), i.e., $E_\alpha - E_s = n\epsilon - E_s$, so that the second term on the rhs of Eq. (2.5) gives

$$\sum_\alpha \exp[-i\omega_{s\alpha}(t-t')]$$

$$= \exp[iE_s(t-t')/\hbar] \sum_n \exp[-i\epsilon/\hbar)(t-t')n]$$

$$= \exp[iE_s(t-t')/\hbar] 2\pi\hbar\rho\delta(t-t'). \tag{3.1}$$

Equation (2.5) now assumes the form

$$-\hbar \dot{a}_s(t) = \pi |V_{\alpha s}|^2 \rho a_s(t) + \pi \sum_{s' \neq s} V_{s\alpha} V_{\alpha s'} \rho \times \exp[it(E_s - E_{s'})/\hbar] a_{s'}(t). \tag{3.2}$$

Equation (3.2), together with Eq. (2.4), results in the dynamics, Eq. (2.14), being characterized by the effective Hamiltonian (2.10), with the decay matrix, Eq. (2.12), being

$$\underset{\approx}{\Gamma}_{ss'} = 2\pi V_{s\alpha} V_{\alpha s'} \rho. \tag{3.3}$$

### B. The random coupling

Random-coupling models have a long history in the theory of nuclear spectra[42] and disordered solids[43] and were applied for the theory of intrastate and interstate dynamics[44] and for the loss of intramolecular coherence in high-order multiphoton excitation and dissociation of polyatomic molecules.[45] In the case of random coupling the sums over the off-diagonal ($s \neq s'$) terms in Eq. (2.5) vanish. In this case the second term on the rhs of Eq. (2.5) vanishes, i.e.,

$$\sum_\alpha V_{s\alpha} V_{\alpha s'} \exp[-i(\omega_{s\alpha} t - \omega_{s'\alpha} t')] \to 0, \tag{3.4}$$

while the diagonal sum, with the help of Eq. (3.1), is

$$\sum_\alpha |V_{s\alpha}|^2 \exp[-i\omega_{s\alpha}(t-t')]$$

$$= \langle |V_{s\alpha}|^2 \rangle \exp[iE_s(t-t')/\hbar] 2\pi\hbar\rho\delta(t-t'), \tag{3.5}$$

where $\langle\rangle$ is defined by Eq. (2.12) and $\rho$ is the (mean) density of states. Equations (2.5) and (3.5) result in

$$-\hbar \dot{a}_s(t) = \pi \langle |V_{s\alpha}|^2 \rangle \rho a_s(t). \tag{3.6}$$

The time evolution of each of the doorway states $\{|s\rangle\}$ is a pure exponential and no coherence effects (quantum beats) are exhibited in the temporal decay of $P(t)$.

### C. Partial correlations

The constant-coupling or the random-coupling models constitute limiting cases. A realistic model system for the level structure, coupling, and accessibility corresponds to a

Franck–Condon system. This consists of zero-order states of two multidimensional harmonic potential surfaces $U_i(q)$ and $U_f(q)$, with the minimum of $U_f(q)$ being considerably lower in energy than that of $U_i(q)$. The eigenstates $\{|\alpha\rangle\}$ of $U_f(q)$ constitute the dissipative quasicontinuum and do not carry oscillator strengths from the ground state $|g\rangle$, representing the Franck–Condon quasicontinuum. The eigenstates $\{|s\rangle\}$ and $U_i(q)$ carry an oscillator strength from $|g\rangle$, constituting the doorway states of the system. The interstate nonadiabatic couplings $V_{s\alpha}$ mix the doorway and quasicontinuum states. From a numerical analysis of the correlations of the $\{|s\rangle\}$–$\{|\alpha\rangle\}$ couplings within the Franck–Condon system (Sec. V) we shall infer that the correlations between the off-diagonal couplings are finite but weak. This state dependence of the off-diagonal couplings will be quantified in terms of the correlation functions

$$\eta_{ss'}=\langle V_{s\alpha}V_{\alpha s'}\rangle/[\langle|V_{s\alpha}|^2\rangle\langle|V_{\alpha s'}|^2\rangle]^{1/2}, \tag{3.7}$$

where $\langle\ \rangle$ is defined by Eq. (2.13) with the energy range $\delta E=d|E_s-E_{s'}|$, with $d=2-5$. The averaged sums over $\alpha$ for the off-diagonal products in Eq. (2.5) then assume the form

$$\left\langle \sum_{\alpha} V_{s\alpha}V_{\alpha s'}\ \exp[-i(\omega_{s\alpha}t-\omega_{s'\alpha}t')]\right\rangle \rightarrow[\langle|V_{s\alpha}|^2\rangle\langle|V_{s'\alpha}|^2\rangle]^{1/2}\eta_{ss'}\ \exp[i(E_st-E_{s'}t')/\hbar]\otimes 2\pi\hbar\rho\,\delta(t-t'). \tag{3.8}$$

The averaging in Eq. (3.8) is taken over an ensemble of systems with different $\eta_{ss'}$ correlations for the coupling.[45] This procedure results in constant values of the squared couplings, which are independent on the specific final state $\alpha$. The resulting equations for the amplitudes are

$$-\hbar\dot{a}_s(t)=\pi\langle|V_{s\alpha}|^2\rangle\rho a_s(t)+\pi\sum_{s'\neq s}[\langle|V_{s\alpha}|^2\rangle\langle|V_{s'\alpha}|^2\rangle]^{1/2}\eta_{ss'}\rho\otimes\exp[(it/\hbar)(E_s-E_{s'})]a_{s'}(t). \tag{3.9}$$

The dynamics, Eq. (3.9), of a system with partial correlations is determined by the effective Hamiltonian (2.10) with the decay matrix

$$\underset{\approx}{\Gamma}_{ss'}=2\pi[\langle|V_{s\alpha}|^2\rangle\langle|V_{s'\alpha}|^2\rangle]^{1/2}\rho\,\eta_{ss'}. \tag{3.10}$$

For the diagonal terms $\eta_{ss}=1$ while for the off-diagonal terms $\eta_{ss'}<1$ with typical values for the Franck–Condon quasicontinuum $\eta_{ss'}\cong 0-0.4$ (Sec. V).

## IV. MODEL CALCULATIONS FOR PARTIAL CORRELATION

From the foregoing analysis of the correlation functions, Eq. (3.7), of the interstate nonadiabatic couplings we infer that the following limiting situations can be realized: $\eta_{ss'}=1$ for constant coupling and $\eta_{ss'}=0$ for random coupling. For the coupling of a doorway state manifold to a Franck–Condon quasicontinuum $\eta_{ss'}<1$, with realistic values (see Sec. V) of $\eta_{ss'}=0.05-0.4$. The latter situation provides a reasonable description of nonadiabatic dynamics in real life. In what follows we shall provide model calculations of temporal vibrational coherence in a model system with partial correlation. These calculations will be supplemented by more detailed simulations (Sec. V) for interstate nonadiabatic dynamics in a Franck–Condon system.

To explore the effects of correlations on the coherent dynamics we considered two doorway states $s=1,2$ with energies $E_1$ and $E_2$ (energy spacing $\Delta E=|E_1-E_2|$) coupled to a common quasicontinuum. We shall use the effective Hamiltonian formalism (Sec. III). The equation of motion of the wave packet $\Psi(t)=A_1(t)|1\rangle+A_2(t)|2\rangle$ is governed by the effective Hamiltonian $(\underset{\approx}{H}_{\rm eff})_{11}=E_1-(i/2)\Gamma_{11}$, $(\underset{\approx}{H}_{\rm eff})_{22}=E_2-(i/2)\Gamma_{22}$ and $(\underset{\approx}{H}_{\rm eff})_{12}=(\underset{\approx}{H}_{\rm eff})_{21}=-(i/2)\,\eta\Gamma_{12}$. For the sake of simplicity we set $\Gamma_{11}=\Gamma_{22}=\Gamma_{12}=\Gamma$ and the initial amplitudes $A_1(0)$ and $A_2(0)$ are taken to be real. Furthermore, we assert that the dominating decay involves the nonradiative channel, as appropriate for femtosecond dynamics, i.e., $\Gamma\gg\Gamma_{\rm rad}$, where $\Gamma_{\rm rad}$ is the radiative width.

The relevant range of the energetic and dynamic parameters, where quantum beats in $P(t)$ are exhibited, is characterized by the number $N_p(=\tau/T_p)$ of the periods $T_p$ $(=h/\Delta E)$ of beats in the decay time domain $\tau(=\hbar/\Gamma)$, which exceeds unity, i.e.,

$$N_p=(2\pi)^{-1}(\Delta E/\Gamma)\geqslant 1, \tag{4.1}$$

so that $\Gamma/\Delta E\leqslant(1/2\pi)$. The time evolution of the system (for $\Gamma/\Delta E<1$), given by Eqs. (2.15) and (2.16), is manifested by the nonradiative population probability, Eq. (2.6), and by the effective rate, Eq. (2.7), which are given by

$$P(t)=\exp(-t/\tau)\left[1-2A_1(0)A_2(0)\left(\frac{\eta\Gamma}{\Delta E}\right)\sin(\Delta Et/\hbar)\right] \tag{4.2}$$

and

$$k(t)=(1/\tau)\left[1+\frac{2\eta A_1(0)A_2(0)\cos(\Delta Et/\hbar)}{1-2A_1(0)A_2(0)\left(\frac{\eta\Gamma}{\Delta E}\right)\sin(\Delta Et/\hbar)}\right]. \tag{4.3}$$

For $\eta\Gamma/\Delta E\ll 1$ this expression reduces to

$$k(t)=(1/\tau)[1+2\eta A_1(0)A_2(0)\cos(\Delta Et/\hbar)]. \tag{4.3a}$$

For the sake of future discussion we also present the photon counting rate, Eq. (2.9), where the transition moments $\mu_{g1}$ and $\mu_{g2}$ are taken to be real. The perturbative result is

$$I(t)\cong\exp(-t/\tau)[|\mu_{g1}A_1(0)|^2+|\mu_{g2}A_2(0)|^2+2\mu_{g1}\mu_{g2}A_1(0)A_2(0)\cos(\Delta Et/\hbar)]. \tag{4.4}$$

It is instructive to note that the amplitude of the leading term of the quantum beats in the nonradiative decay probability $P(t)$, Eq. (4.2), and in the effective rate $k(t)$, Eq. (4.3), is determined by the correlation parameter $\eta$, in contrast to the quantum beats contribution to $I(t)$, Eq. (4.4), whose amplitude is independent of $\eta$.

Figure 2 presents typical results based on Eqs. (2.6), (2.7), (2.15), and (2.16) for $P(t)$ and $k(t)$ in a model system

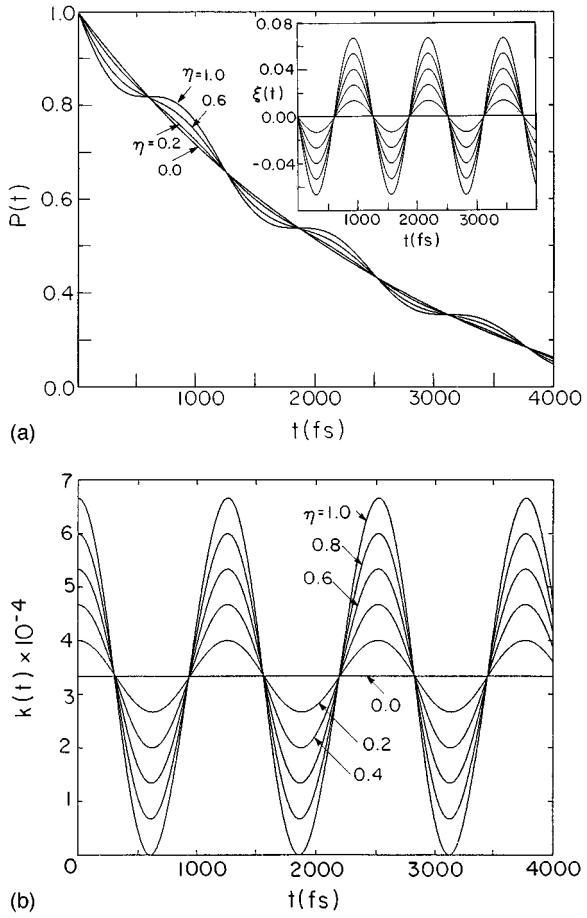


FIG. 2. Model calculations for the reactants population probability $P(t)$ within the framework of the modulation amplitudes $\xi(t)$, Eq. (4.1), and the effective rate $k(t)$ of the effective Hamiltonian formalism for the decay of a wave packet of two doorway states $|1\rangle$ and $|2\rangle$ with $E_1-E_2=26.5\ \mathrm{cm}^{-1}$, $\Psi(t)=A_1(t)|1\rangle+A_2(t)|2\rangle$ $(A_1(0)=A_2(0)=1/\sqrt{2})$ to a quasicontinuum. The quasicontinuum is characterized by the decay matrix $\Gamma_{11}=\Gamma_{22}=\Gamma$ and $\Gamma_{12}=\eta\Gamma$, with $\Gamma=1.77\ \mathrm{cm}^{-1}$ and $\eta=0-1$ (marked on the curves). (a) Calculation of $P(t)$. The insert shows the values of $\xi(t)$ for increasing values of $\eta=1.0$ (highest modulation) to $\eta=0$ (flat line) in steps of 0.2. (b) Calculation of $k(t)$.

for the energetic and dynamic parameters $\Delta E=26.5\ \mathrm{cm}^{-1}$ and $\tau\equiv\hbar/\Gamma=3000$ fs $(\Gamma=1.77\ \mathrm{cm}^{-1})$, and for the initial conditions $A1(0)=A2(0)=1/\sqrt{2}$, while the correlation parameter was taken in the range $\eta=0-1$. From Eqs. (4.2) and (4.3) and the model calculations portrayed in Fig. 2 we infer the following.

(1) For the random coupling limit, i.e., $\eta=0$, a pure exponential decay of $P(t)=\exp(-t/\tau)$ is exhibited with a constant effective rate $k=1/\tau$. No modulation of $P(t)$ and of $k(t)$ is exhibited.

(2) For correlated coupling, i.e., $0<\eta<1$, temporal modulation of $P(t)$ and of $k(t)$ is exhibited. The temporal modulation is characterized by the period $T_p=h/\Delta E$, with $T_p$ being independent of $\eta$, as expected.[32] The amplitude of the temporal modulation increases linearly with increasing $\eta$.

(3) For the constant coupling limit $\eta=1$, the most pronounced temporal modulation amplitudes of $P(t)$ and of $k(t)$ are exhibited.

(4) In general, the population probability of the reactants $P(t)$, Eq. (4.2), and the population probability of the products $P_\alpha(t)$, Eq. (2.8), are characterized by weak modulation amplitudes. The modulation amplitudes of $P(t)$ can be characterized by

$$\xi(t)=\frac{P(t)-Av[P(t)]}{Av[P(t)]}, \tag{4.5}$$

where $Av[P(t)]$ represented the smoothened $P(t)$ curve (which corresponds to $\eta=0$ with the same parameters). A maximal value $|\xi^{(\eta)}|$ of the modulation amplitudes of $P(t)$ for a given value of $\eta$, is given from Eq. (4.2) by the simple [perturbative] result

$$|\xi^{(\eta)}|=\eta(\Gamma/\Delta E). \tag{4.6}$$

The data of Figs. 2 and 3 (which give $|\xi^{(\eta=1)}|=0.07$ and $|\xi^{(\eta=0.2)}|=0.015$), which correspond to $(\Delta E/\Gamma)=15$, are in agreement with these results. From Eq. (4.6) we conclude that for the relevant range of $(\Delta E/\Gamma)(\geqslant 2\pi)$, the maximal values of the modulation amplitudes (for $\eta=1$) are given by $|\xi^{(\eta=1)}|=(\Gamma/\Delta E)\ll 1$. The $\eta$ dependence of the modulation amplitude is linear, i.e., $|\xi^{(\eta)}|\propto\eta$, exhibiting a marked decrease for weak correlations. For a Franck–Condon system (Sec. V) $\eta=0.4-0.05$ and the temporal modulations of $P(t)$ are diminished.

(5) The temporal modulation of the effective rate $k(t)$ is considerably larger than that of $P(t)$. The modulation amplitudes of $k(t)$ can be expressed by

$$\varphi(t)=\frac{k(t)-Av[k(t)]}{Av[k(t)]}. \tag{4.7}$$

A maximal value $|\varphi^{(\eta)}|$ of the amplitude modulation of $k(t)$ for a given value of $\eta$ is given from Eq. (4.3) by

$$|\varphi^{(\eta)}|=\eta. \tag{4.8}$$

For lower values of $\eta$ the modulation of $k(t)$ decreases linearly with $\eta$. The modulation of $k(t)$ is independent of $\Delta E/\Gamma$. In particular for $\eta=1$ complete interference is exhibited for $k(t)$, with $k(t)$ reaching the value of zero when $\varphi(t)=-1.0$, while for lower values of the correlation parameter $\eta$ the values of $|\varphi(t)|$ diminish linearly with decreasing $\eta$.

For lower values of $N_p<1$, $P(t)$ does not involve quantum beats, but rather the decay of overlapping resonances,[46] which will be explored in a future work.[46(c)] The model calculations for partial correlation rest on an oversimplified description of the dissipative quasicontinuum (which is characterized by the parameter $\Gamma$), which will now be extended to consider dynamics in a Franck–Condon system.

## V. DYNAMICS IN THE FRANCK–CONDON QUASICONTINUUM

The Franck–Condon system (Fig. 1) is characterized by the doorway states $\{|s\rangle\}$ of a harmonic potential surface $U_i(q)$, which are coupled to the manifold of the final states $\{|\alpha\rangle\}$ of a potential surface $U_f(q)$. The minimum of $U_f(q)$ is considerably lower in energy than the $U_i(q)$, so that the

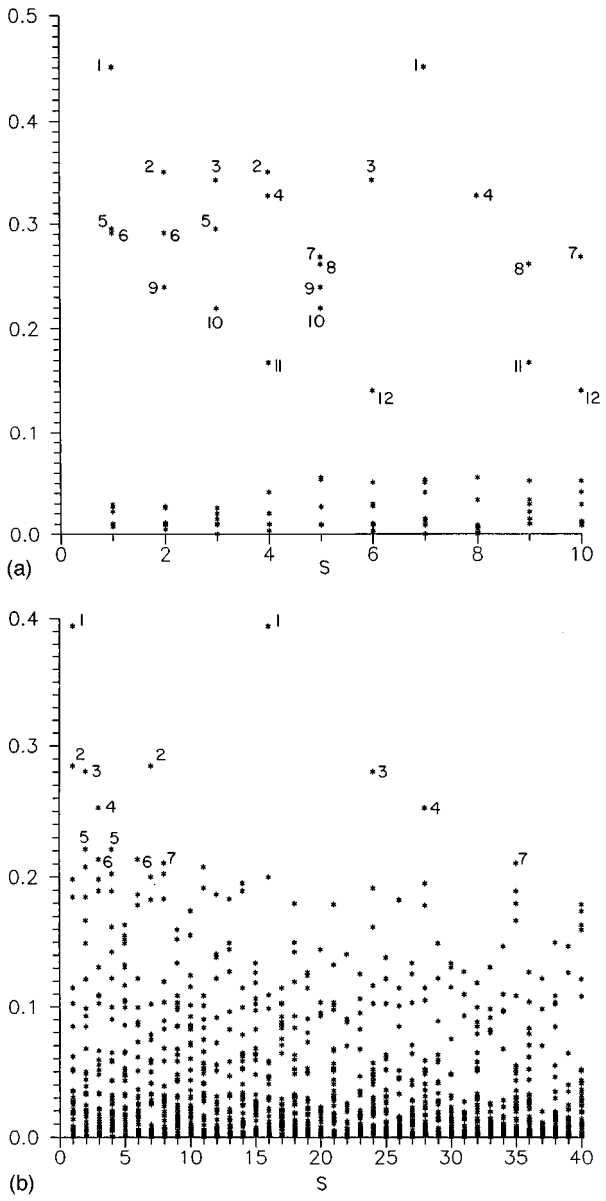


FIG. 3. Absolute values of the correlation parameters $|\eta_{ss'}|$, Eq. (5.12), between doorway states $s,s'$. Data for the four-mode Franck–Condon system with the frequencies $\nu_1=27\ \mathrm{cm}^{-1}$, $\nu_2=35\ \mathrm{cm}^{-1}$, $\nu_3=75\ \mathrm{cm}^{-1}$, $\nu_4=117\ \mathrm{cm}^{-1}$, with the coupling parameters are specified in Sec. V. The $s$ and $s'$ states are labeled by the index $s=1,2,3,\ldots,N$ in the order of increasing energy. Each $s$ state is correlated with the states $s'=1,\ldots,N$ and vice versa, so that for each $s,s'$ two identical correlation parameters $\eta_{ss'}$ and $\eta_{s's}$ are presented (which allow for the easy identification of $s$ and $s'$). The larger correlation parameters are labeled by numbers, which represent the corresponding values of $s$ and $s'$, each labeled by the combination of the quantum numbers $\Sigma_j\kappa_j\omega_j$ ($j=1-4$ and $\kappa_j$ are integers) and being given by $s,s'=[\Sigma_j\kappa_j\omega_j,\Sigma_j\kappa_j'\omega_j']$, while 0 corresponds to the electronic origin. (a) $\Delta E=500\ \mathrm{cm}^{-1}$. The energy range $\Delta E-50\ \mathrm{cm}^{-1}\leqslant E\leqslant\Delta E+250\ \mathrm{cm}^{-1}$ contains $N=10$ states and 90 values of $\eta_{ss'}$. The pairs of states with the largest values of $\eta_{ss'}(>0.1)$, which are labeled as 1–12, are: 1. $[0,\nu_3]$, 2. $[\nu_1,\nu 2_1]$, 3. $[\nu_2,2\nu_2]$, 4. $[2\nu_1,3\nu_1]$, 5. $[0,\nu_2]$, 6. $[0,\nu_1]$, 7. $[\nu_1+\nu_2,2\nu_1,\nu_2]$, 8. $[\nu_1+\nu_2,\nu_1+2\nu_2]$, 9. $[\nu_1,\nu_1+\nu_2]$, 10. $[\nu_2,\nu_1+\nu_2]$, 11. $[2\nu_1,2\nu_1+\nu_2]$, 12. $[2\nu_2,2\nu_2+\nu_1]$. (b) $\Delta E=500\ \mathrm{cm}^{-1}$. The energy range $\Delta E-200\ \mathrm{cm}^{-1}\leqslant E\leqslant\Delta E+250\ \mathrm{cm}^{-1}$ contains $N=40$ states and 1560 values of $\eta_{ss'}$. The pairs of states with the largest values of ($\eta_{ss'}>0.2$), which are labeled as 1–7, are: 1. $[0,\nu_4]$, 2. $[0,\nu_3]$, 3. $[\nu_1,\nu_1+\nu_4]$, 4. $[\nu_2,\nu_2+\nu_4]$, 5. $[\nu_1,2\nu_1]$, 6. $[\nu_2,2\nu_2]$, 7. $[3\nu_1,3\nu_1+\nu_4]$.

$\{|\alpha\rangle\}$ manifold constitutes a dissipative quasicontinuum. The zero-order states are characterized by the doorway states $\{|s\rangle\}=\{\phi_i\chi_s\}$ and the quasicontinuum states $\{|\alpha\rangle\}=\{\phi_f\chi_\alpha\}$, where $\phi_i$ and $\phi_f$ denote the electronic wave function of the initial and the final manifolds, respectively. $\chi_s$ and $\chi_\alpha$ denote the nuclear wave functions. The coupling terms are:

$$V_{s\alpha}=Vf(s;\alpha), \tag{5.1}$$

$$f(s;\alpha)=\langle\chi_s|\chi_\alpha\rangle, \tag{5.2}$$

where $V$ is the electronic coupling (within the framework of the Condon approximation) and $f(s;\alpha)$ is the vibrational overlap integral.

In what follows we consider explicitly the entire level structure of the system. The Hamiltonian $\underset{\approx}{H}$ of the system, Eq. (2.1), is diagonalized by the unitary transformation $\underset{\approx}{U}\underset{\approx}{H}\underset{\approx}{U}^{+}=\underset{\approx}{E}$, resulting in the molecular eigenstates

$$|j\rangle=\sum_s a_s^{(j)}|s\rangle+\sum_\alpha b_\alpha^{(j)}|\alpha\rangle, \tag{5.3}$$

where $a_s^{(j)}=U_{js}$ and $b_\alpha^{(j)}=U_{j\alpha}$. The energies $E_j$ of the molecular eigenstates constitute the diagonal elements of $\underset{\approx}{E}$. The zero-order vibronic states can be reconstructed from the molecular eigenstates

$$\begin{aligned}|m\rangle&=\sum_j (U^{+})_{mj}|j\rangle,\\ &=\sum_j c_m^{(j)}|j\rangle\end{aligned}$$

$$(c_m^{(j)}=a_s^{(j)}\quad\text{for } m=s,\quad c_m^{(j)}=b_\alpha^{(j)}\quad\text{for } m=\alpha). \tag{5.4}$$

The initial state, Eq. (2.2), is expressed in the form

$$\Psi(0)=\sum_s\sum_j A_s(0)a_s^{(j)}|j\rangle. \tag{5.5}$$

Eq. (5.5) provides the transformation from a wave packet of zero-order doorway states to a wave packet of molecular eigenstates, which provides the time evolution

$$\Psi(t)=\sum_s\sum_j A_s(0)a_s^{(j)}|j\rangle\exp(-iE_jt/\hbar). \tag{5.6}$$

The population probability of the reactant doorway states, Eq. (2.6), is obtained from Eq. (5.6) in the form

$$\begin{aligned}P(t)&=\sum_{s'}\left|\sum_s\sum_j A_s(0)a_s^{(j)}a_{s'}^{(j)}\exp(-iE_jt/\hbar)\right|^2\\ &=\sum_{s'}\left[\left|\sum_s A_s(0)S_{ss'}(t)\right|^2+\left|\sum_s A_s(0)C_{ss'}(t)\right|^2\right],\end{aligned} \tag{5.7}$$

where

$$S_{ss'}(t)=\sum_j a_s^{(j)}a_{s'}^{(j)}\sin\left(\frac{E_jt}{\hbar}\right), \tag{5.8a}$$

$$C_{ss'}(t)=\sum_j a_s^{(j)}a_{s'}^{(j)}\cos\left(\frac{E_j t}{\hbar}\right). \tag{5.8b}$$

Equations (5.7) and (5.8) provide the information on coherent dynamics. We now proceed to characterize the harmonic manifolds $\{|s\rangle\}$ and $\{|\alpha\rangle\}$ and their couplings $V_{s\alpha}$, Eq. (5.1), within the framework of the harmonic model.

The level structure and coupling within the Franck–Condon model will be described by a simple harmonic model with two multidimensional displaced nuclear potential surfaces $U_i(\mathbf{q})$ and $U_f(\mathbf{q})$, which are characterized by the same frequencies. The relevant $n$ vibrational modes are characterized by coordinates $\mathbf{q}\equiv\{q_1,q_2,\ldots,q_n\}$, masses $\mathbf{m}\equiv\{m_1,m_2,\ldots,m_n\}$, frequencies $\boldsymbol{\omega}\equiv\{\omega_1,\omega_2,\ldots,\omega_n\}$, and displacements of the equilibrium positions between the minima of the potential surfaces $\Delta\mathbf{q}\equiv\{\Delta q_1,\Delta q_2,\ldots,\Delta q_n\}$. It is useful to define the squares of the reduced displacements $S_k=\Delta q_k^2 m_k\omega_k/2\hbar$. The nuclear reorganization energy is

$$\lambda=\sum_{k=1}^{n}\hbar\omega_k S_k \tag{5.9}$$

and the energy gap between the minima of the two potential surfaces is denoted by $\Delta E$. The initial and final vibronic states will be specified in terms of the occupation numbers of the vibrational modes, i.e., $|s\rangle\equiv\{i_1,i_2,\ldots,i_n\}$ and $|\alpha\rangle\equiv\{f_1,f_2,\ldots,f_n\}$, respectively.

The vibrational overlap between the initial $i_k$ and final $f_k$ states of the model is

$$f(i_k;f_k)=\exp(-S/2)(i!f!)^{1/2}\times\sum_{r=0}^{\min(i,f)}\frac{(-1)^{i+f-r}S^{(i+f-2r)/2}}{r!(i-r)!(f-r)!}, \tag{5.10}$$

where on the rhs of Eq. (5.10) we abbreviate $S\equiv S_k$, $i\equiv i_k$, and $f\equiv f_k$. The Franck–Condon vibrational overlaps between the vibronic states $|s\rangle$ and $|\alpha\rangle$ are

$$f(s,\alpha)=\prod_{k=1}^{n}f(i_k;f_k). \tag{5.11}$$

We have performed numerical model calculations for the level structure coupling and dynamics in a four-mode harmonic model of two displaced potential surfaces. The input data are the harmonic modes frequencies $\underset{\sim}{\omega}=(\omega_n,\omega_{n-1},\ldots,\omega_1)$ (with the $\omega_j$'s being given in the order of increasing frequency), the reduced displacements parameters $\underset{\sim}{S}=(S_1,S_2,\ldots,S_n)$, the energy gap $\Delta E$ between the minima of $U_f$ and $U_i$ ($\Delta E=U_f-U_i$), and the electronic coupling $V$.

The input parameters taken for our model calculations were $\underset{\sim}{\omega}/\mathrm{cm}^{-1}=(117, 75, 35, 27)$, and $\underset{\sim}{S}=(1.0, 1.1, 2.0, 3.0)$, which give $\lambda=350\ \mathrm{cm}^{-1}$, and the energy gap $\Delta E=500\ \mathrm{cm}^{-1}$. The highest vibrational mode is close to the intermolecular vibrational motion in the $D$–$A$ charge transfer complex, while the lower vibrational frequencies mimic solvent modes. The electronic coupling was chosen as $V=20\ \mathrm{cm}^{-1}$, to give ultrafast dynamics on the time scale $\tau_d\sim1500$ fs. The choice of the energy parameters was guided by the following constraints: (i) attainment of a vibrational quasicontinuum $\Delta E\gg\omega_f$ for all the vibrational frequencies, (ii) negligible edge effects, i.e., $\Delta E\gg 2\pi V^2\ \mathrm{FD}(E_s)$ for all the doorway states, and (iii) the direct decay is slower than the coherent modulation frequency, i.e., $2\pi V^2\ \mathrm{FD}(E_s)\sim 2\pi V^2\ \mathrm{FD}(E_{s'})\leqslant(E_s-E_{s'})$. Here $\mathrm{FD}(E_s)$ is the Franck–Condon density[47] around $E_s$, i.e., $\mathrm{FD}(E_s)=[\delta E]^{-1}\Sigma_\alpha|f(s;\alpha)|^2$, where the $\alpha$ sum is taken over the quasicontinuum states in the energy range $E_s-\delta E/2\leqslant E_\alpha\leqslant E_s+\delta E/2$.

The zero-order basis set consists of $n_s(=100)$ doorway states $\{|s\rangle\}$ and $n_\alpha(=3000)$ quasicontinuum states. The $(n_s+n_\alpha)\times(n_s+n_\alpha)$ Hamiltonian matrices were diagonalized resulting in the molecular eigenstates $\{|j\rangle\}$ with the accessibility amplitudes $\{a_s^{(j)}\}$ and the energies $\{E_j\}$. The temporal decay of a wave packet of doorway states was simulated using Eqs. (5.7) and (5.8).

Regarding the input data, of considerable interest are the correlation functions $\eta_{ss}$, Eq. (3.10), for the coupling to the Franck–Condon quasicontinuum. Using Eq. (5.1) these correlations are

$$\eta_{ss'}=\frac{\langle f(s;\alpha)f(\alpha;s')\rangle}{[\langle f(s;\alpha)^2\rangle\langle f(s';\alpha)^2\rangle]^{1/2}}. \tag{5.12}$$

Numerical calculations of $\eta_{ss'}$ for $s,s'=1-10$ and $s,s'=1-40$ (where $s=1$ denoted the electronic origin) were performed. Figure 3 portrays the absolute values of $|\eta_{ss'}|$. The values of $|\eta_{ss'}|$ show some dependence on the range of $\delta E$ over which the averaging is performed. For a fixed value of the lower limit of $\delta E$ the values of $\eta_{ss'}$ show a weak dependence (10%) on the upper limit of $\delta E$ (in the range $\delta E+\Delta E=\nu_j d_j$, where $d_j=1.5-8$, $\nu_j$ being the characteristic frequencies and $\Delta E$ being the electronic origin energy of the $\{|s\rangle\}$ manifold). The $\eta_{ss'}$ show a more pronounced sensitivity (in the variance range of $\sim50\%$) on the lower limit of the energy domain (in the range $\Delta E-\delta E=\nu_j d_j$ with $d_j=0.5-8$). The relative sizes of the largest values of $\eta_{ss'}$ ($>0.1$) are practically invariant with respect to the lower limit of the energy range $\delta E$. As the calculations of the $\eta_{ss'}$ are intended to demonstrate the nature of the correlation effects between doorway states, this variance of the values of $\eta_{ss'}$ is of little concern. The (absolute values of) correlation parameters $|\eta_{ss'}|$ for pairs $(s,s')$ of doorway states [Figs. 3(a) and 3(b)] are considerably lower than unity. The highest values of correlation parameters fall in the region $\eta_{ss'}=0.4-0.2$. These relatively high values of $|\eta_{ss'}|$ correspond to members of a vibrational progression with $s$ and $s'$ differing only by a single vibrational quantum (Fig. 3) i.e., $\Delta v_j=\pm1$ (where $v_j$ is the vibrational quantum number of mode $j$), with the highest value of $|\eta_{ss'}|$ being $\sim0.4$. For multimode changes between $s$ and $s'$ very low values of $|\eta_{ss'}|$ are exhibited. From this analysis we infer that weak, but nonvanishing, correlations, which are subjected to propensity rules, do exist for the coupling of a manifold of doorway states to a Franck–Condon quasicontinuum. These finite correlations will preserve some temporal interference effects

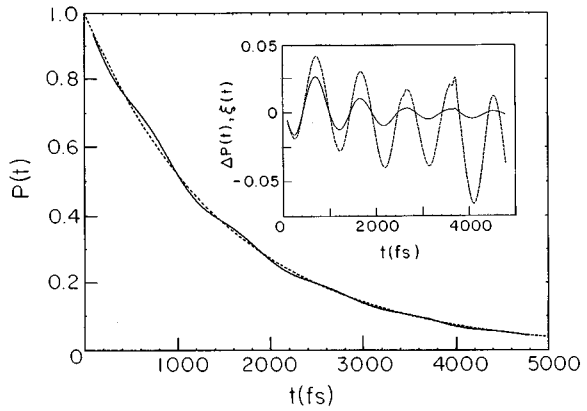


FIG. 4. The time-dependent population probability of the reactants $P(t)$ for the decay of the two-doorway states initial wave packet $\Psi(0)=|1\rangle+|2\rangle$ defined in the text (the solid line). The dashed line shows $Av[P(t)]$. The insert shows the time dependence of $\Delta P(t)=P(t)-Av[P(t)]$ (the solid line) and of $\xi(t)$, Eq. (4.1) (the dashed line).

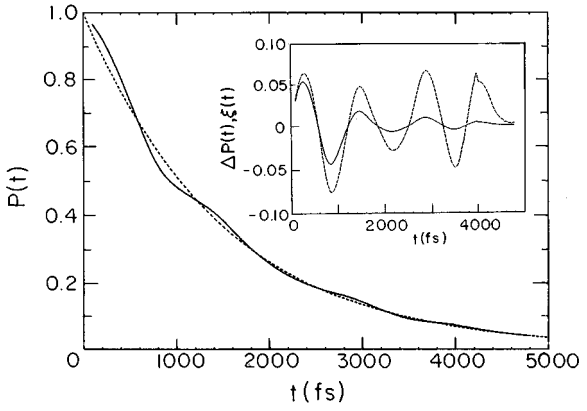


FIG. 6. The time-dependent population probability $P(t)$ of the reactants for the seven-doorway states initial wave packet $\Psi(0)=\underset{\sim}{A}_s(0)|\underset{\sim}{s}\rangle^+$ defined in the text (the solid line). The dashed line shows $Av[P(t)]$. The insert shows the time dependence of $\Delta(P)=P(t)-Av[P(t)]$ (the solid line) and of $\xi(t)$, Eq. (4.1) (the dashed line).

in the dynamics. The present estimates of $|\eta_{ss'}|\lesssim 0.4$ were already utilized in Sec. IV for simple modeling of quantum beats.

We now utilize the complete numerical information on the molecular eigenstates and the initial conditions for the wave packet expressed by $\underset{\sim}{A}_s(0)$, together with Eqs. (5.7) and (5.8), for the numerical calculation of the time-resolved dynamics. Typical data for the time-dependent reactants decay probability $P(t)$ are presented in Figs. 5 and 6. $P(t)$ for the decay of the initial wave packet of two states $\Psi(0)=|0\rangle+|1\rangle$, where $|0\rangle$ is the electronic origin and $|1\rangle=|\nu_1\rangle=27\ \mathrm{cm}^{-1}$ is the single vibrational excitation (Figs. 4 and 5) exhibits regular, but weak, temporal coherence with the single period and with the largest modulation amplitude $|\xi(t)|\cong 0.042$ (insert to Fig. 4). This largest modulation amplitude of $|\xi|=0.042$ is in good agreement with the analysis of the model system in Sec. IV. For this two-doorway states system (Fig. 5) $\tau=1900$ fs ($\Gamma=2.8\ \mathrm{cm}^{-1}$) and $\Gamma/\Delta E=0.103$, so that Eq. (4.6) (i.e., $|\xi^{\eta}|\cong 0.103|\eta|$) accounts for these data with the reasonable correlation parameter $|\eta|=0.4$ [while the numerical value of the $[0,\nu_4=27\ \mathrm{cm}^{-1}]$ correlation parameter in Fig. 3(a) is $\eta=0.29$]. These low $|\xi(t)|$ values originate from an intrinsically small contribution to the off-diagonal matrix elements of the nonradiative decay matrix, i.e., $\sim\Gamma/\Delta E$ according to Eq. (4.6), in conjunction with low value(s) of correlation parameters. For this two-doorway states system $k(t)$ shows a more pronounced modulation with the largest modulation amplitude of $|\varphi(t)|=0.4$ (Fig. 5), which is still considerably lower than the maximal value of unity, reflecting the reduction of $\eta$, according to Eq. (4.8). In Figs. 6 and 7 we display the dynamics of a multistate wave packet initially containing the seven lowest states in the $\{|s>\}$ manifold and spanning the energy range of $75\ \mathrm{cm}^{-1}$, i.e., $\Psi(0)=\underset{\sim}{A}_s(0)|\underset{\sim}{s}\rangle$, where $|\underset{\sim}{s}\rangle=(0,\nu_1,\nu_2,2\nu_1,\nu_1+\nu_2,2\nu_2,\nu_3)$, with the amplitudes which are given by the vibrational overlap integrals from the electric origin of the lowest manifold, i.e., $\underset{\sim}{A}_s(0)=(0.0287,-0.0498,-0.0406,0.0609,0.0704,0.0406,-0.0301)$. These data show a somewhat less regular modulation with the largest values of $|\xi(t)|$ ($=0.06$ for the maximal value of

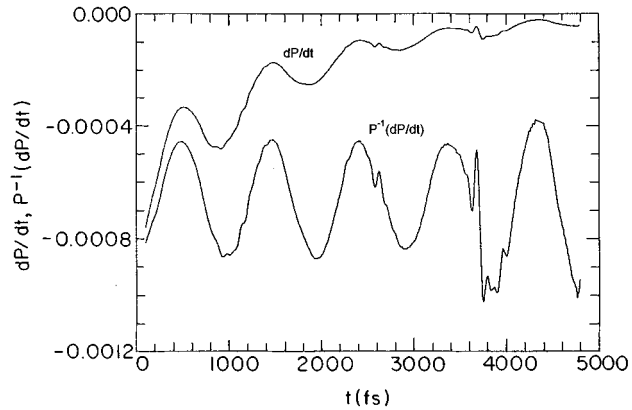


FIG. 5. The time dependence of $\dot{P}(t)$ (upper curve) and of $-k(t)=P(t)^{-1}\dot{P}$ (lower curve) for the dynamics of the two-doorway states system of Fig. 4.

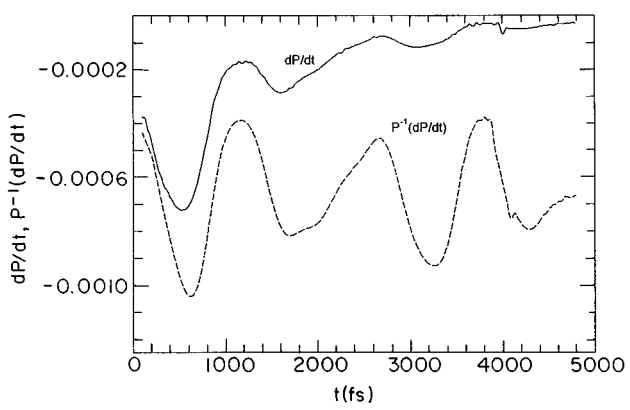


FIG. 7. The time dependence of $\dot{P}(t)$ (upper curve) and of $k(t)=P(t)^{-1}\dot{P}(t)$ (lower curve) for the dynamics of the seven-doorway states system of Fig. 6.

Fig. 5) and of $|\varphi(t)|$ ($=0.33$ for the maximal value). The time-resolved reactants, which decay into a typical Franck–Condon quasicontinuum, exhibit modest effects on the temporal modulation, with maximal values of the modulation amplitudes, Eq. (4.5), of $|\xi(t)| \sim 0.04-0.06$, which are close to the $|\xi(t)|$ values obtained for the two-doorway states system. A more pronounced effect of temporal coherence is exhibited for the (time-dependent) decay rate $k(t)$, with a maximal modulation amplitude of $|\varphi(t)| \cong 0.3-0.4$, which is considerably lower than the upper limit of unity (for $|\eta_{ss'}|=1$), reflecting [according to Eq. (4.8)] the effects of the low correlation parameters. A cursory comparison of these results for the Franck–Condon quasicontinuum with the model calculations, based on the effective Hamiltonian formalism (Sec. IV), indicates that the Franck–Condon system is characterized by weak correlation, i.e., $\eta_{ss'} \leqslant 0.4$. This conclusion concurs with the direct analysis of $\eta_{ss'}$ (Fig. 3). For nonadiabatic dynamics the temporal modulation for the reactants and products is of the same form, as is evident from Eqs. (2.6) and (2.8).

## VI. CONCLUDING REMARKS

We explored temporal vibrational coherence effects in nonadiabatic radiationless transitions between two electronic states in a large molecule or in the condensed phase. The nonadiabatic time-resolved dynamics is determined by the microscopic rates (the diagonal elements of the decay matrix)

$$k_s = 2\pi V^2 F D(E_s)/\hbar, \tag{6.1}$$

while the off-diagonal matrix elements of the decay matrix, Eq. (3.10), are

$$\Gamma_{ss'} = \eta_{ss'}(\hbar/2)(k_s k_{s'})^{1/2}. \tag{6.2}$$

The time dependence of the nonradiative decay probability is obtained from Eqs. (2.6), (2.15), and (2.16) (for the limit of interest when quantum beats are manifested, i.e., $\Gamma_{ss'} \ll |E_s - E_{s'}|$) in the form

$$P(t) \cong \sum_{\{s\}} |A_s(0)|^2 \exp(-k_s t) + \sum_{\{s\}\neq\{s'\}}\sum A_s^* A_{s'}\left[\frac{i\hbar\,\eta_{ss'}(k_s k_{s'})^{1/2}}{2(E_s - E_{s'})}\right] \otimes [\exp(i(E_s - E_{s'}))t/\hbar]\exp[-(k_s + k_{s'})t/2], \tag{6.3}$$

where $\{s\}=|s\rangle,|s'\rangle,\ldots$, represent the doorway states within the laser bandwidth. The first term in Eq. (4.3) represents dynamics of population changes of the doorway states while the second term denotes the coherence effects. Another pertinent observable is the photon counting rate, Eqs. (2.9), (2.15), and (2.16) (for $|E_s - E_{s'}| \gg \Gamma_{ss'} \gg \Gamma_{\mathrm{rad}}$) which is

$$I(t) = \sum_{\{s\}} |A_s(0)|^2 |\mu_{\mathrm{gs}}|^2 \exp(-k_s t) + \sum_{\{s\}\neq\{s'\}}\sum A_s^*(0) A_{s'}(0)\mu_{\mathrm{gs}}^*\mu_{\mathrm{gs}'} \otimes \exp[i(E_s - E_{s'})t]\exp[-(k_s + k_{s'})t/2]. \tag{6.4}$$

On the basis of these results we address the following issues:

(1) How are quantum beats manifested in the time dependence of different observables, i.e., nonradiative population probabilities and photon counting rates? While the periods $T_p = h/|E_s - E_{s'}|$ of the quantum beats are, of course, invariant for the nonradiative and radiative decay, their amplitudes qualitatively and quantitatively differ for the nonradiative and for the radiative decay channels. As is apparent from Eqs. (6.3) and (6.4) two major differences between $P(t)$ and $I(t)$ emerge. First, as noted in Sec. II and as is apparent from Eqs. (4.2), (4.3), and (4.4) for a simple model system of two-doorway states, as well as from Eqs. (6.3) and (6.4), the amplitude of the temporal interference terms is much larger for the rates $I(t)$ or $k(t)$ than for the population probability $P(t)$. For $P(t)$ the amplitude ratios for the quantum beats [i.e., the ratios of the amplitudes in the second term and in the first term in Eq. (6.3)] are $\Gamma_{ss'}/|E_s - E_{s'}| \ll 1$, while the ratio of the amplitudes for the quantum beats for $I(t)$, Eq. (6.4), are of the order of unity. Second, the amplitudes of the temporal coherence terms for the nonradiative probability, Eq. (6.3), are determined by the molecular or condensed phase parameters for nonradiative coupling and relaxation $\eta_{ss}(k_s k_{s'})^{1/2}$, while the amplitudes of the temporal coherence terms in the radiative decay rate are determined by the products of the $\mu_{\mathrm{gs}}^*\mu_{\mathrm{gs}'}$ and do not depend on the nonradiative parameters. The radiative decay rate $I(t)$ of a wave packet of doorway states into a radiative continuum is characterized by complete correlation (i.e., $\eta_{ss'}=1$ for all $s,s'$), while the nonradiative decay of such a wave packet into a Franck–Condon quasicontinuum is subjected only to partial intramolecular correlations ($\eta_{ss'} \leqslant 0.4$), further reducing the modulation amplitudes for $P(t)$ and $k(t)$ in the nonradiative decay. It is important to realize that the low modulation amplitudes in coherent nonradiative decay reflect the intramolecular correlation effects, while the large modulation amplitudes in the radiative decay just manifest the signature of the ''preparation'' conditions. While the quantum beats in the radiative decay rate are much more pronounced than for the nonradiative probability, the latter is much more interesting, manifesting information on nonradiative correlation effects, while the former just provides spectroscopic information for the energy differences $|E_s - E_{s'}|$. Thus novel dynamic information emerges from the (weak) quantum beats in the nonradiative population probability, but not from the photon counting rate.

(2) What determines the characteristics of quantum beats for the nonradiative decay of an (initial) wave packet of doorway states into a Franck–Condon quasicontinuum? The manifestation of the quantum beat terms in $P(t)$ is determined by the spectroscopic, energetic, and dynamic properties of the doorway states (within the laser bandwidth) $|s\rangle,|s'\rangle,|s''\rangle,\ldots$, which are characterized by: (i) large preparation amplitudes $A_s(0)$, $A_{s'}(0),\ldots$, for excitation from the ground state; (ii) the periods $T_p = h/|E_s - E_{s'}|$, according to relation (6.3), i.e., $\tau/T_p \geqslant 1$; (iii) modulation amplitudes determined by $\Gamma_{ss'}/|E_s - E_{s'}| \sim (\hbar/2)\eta_{ss'}(k_s k_{s'})^{1/2}/|E_s - E_{s'}|$, where $\Gamma_{ss'}$ is the off-diagonal matrix element of the nonradiative decay matrix, which is proportional to $\eta_{ss'}$,

and (iv) sufficiently large values of the correlation parameters $\eta_{ss'}$, which constitute a novel feature of the Franck–Condon quasicontinuum. While features (i) and (ii) provide the signature of the laser excitation (''preparation'') conditions, features (iii) and (iv) constitute intrinsic properties of the nonadiabatic nonradiative coupling and dynamics. Our analysis provides the distinction between the experimental conditions of wave packet ''preparation,'' which reflect the level structure and ''excitation'' amplitudes of doorway states, and the intrinsic aspects of intramolecular coupling and dynamics, as manifested in the amplitudes of the quantum beats for nonradiative decay.

(3) What are the general properties of the Franck–Condon quasicontinuum? This central issue, which pertains to the features of the correlation parameters introduced and explored herein, transcends the problem of quantum beats and addresses broad features of intramolecular and condensed phase radiationless transitions. From the point of view of general methodology, the most significant result is the occurrence of finite, though low, correlations for the coupling of the manifold of doorway states into a Franck–Condon quasicontinuum (i.e., $\eta_{ss'} \leqslant 0.4$), in contrast to the idealized model system of constant coupling[41] ($\eta_{ss}=1$) and of random coupling[44,45] ($\eta_{ss'}=0$). These finite correlations ensure the realization of nonvanishing off-diagonal matrix elements of the decay matrix $\underset{\sim}{\Gamma}$, Eq. (3.10), resulting in quantum beats in the temporal nonradiative decay of an initially prepared wavepacket of doorway states.

(4) Does a coherent excitation of a wave packet of doorway states modify the nonadiabatic ET dynamics? The answer to this question rests on the nature of the temporal modulation and on its magnitude for a given dynamic observable. Only when the temporal modulation amplitudes depend on the molecular or condensed phase parameters for nonradiative coupling can we assert that the quantum beats in the dynamic variable modify the nonadiabatic dynamics. This is the case for the nonradiative population probability $P(t)$. The temporal modulation amplitudes in $P(t)$ are weak $\sim \Gamma_{ss'}/|E_s - E_{s'}|$, as is apparent from a cursory examination of Figs. 2(a), 4, and 6. Thus, the overall influence of the coherent excitation on the nonradiative dynamics is small. On the other hand, the amplitudes of the pronounced quantum beats in the photon counting rate $I(t)$ do not provide information on nonradiative coupling, just reflecting radiative interference effects. Vibrational coherence effects in the electronically excited bacteriochlorophyll dimer ($^1P^*$) of the bacterial photosynthetic reaction center were experimentally studied by induced and spontaneous fluorescence,[27] i.e., by the interrogation of $I(t)$. These quantum beats in $I(t)$ just provide spectroscopic-type information on the excitation amplitudes $\{A,(0)\}$ within the laser bandwidth and the energy gaps $|E_s - E_{s'}|$ of the doorway states, while the primary charge separation dynamics [determined by the microscopic rates $k_s$, Eq. (6.1)] is unmodified by the coherent excitation of the wavepacket of doorway states.

We have performed model calculations for the time-resolved nonradiative decay of an initially prepared wave packet of doorway states into a Franck–Condon quasicontinuum, based on the dynamics of wave packets for a realistic Franck–Condon level structure, which originates from coupling between two coupled manifolds of zero-order harmonic states. Our treatment rests, in principle, on the exact diagonalization of the entire Hamiltonian of the system, without considering a separation of the relevant system from the bath. In practice we treated a four-mode system, while other degrees of freedom (which can be considered as a bath) (which will contribute to relaxation and ''dephasing'') were not taken into account. Indeed, a four-mode (harmonic) system is of sufficient size to provide relevant information on vibrational coherence effects in nonradiative decay. Regarding additional hidden assumptions in our treatment, we note that an additional effect not considered by us, which may diminish the modulation amplitudes in real life, pertains to static inhomogeneous broadening effects on the energy differences $|E_s - E_{s'}|$ between doorway states. In addition, coherent excitation of a large number of low frequency vibrational modes, as is the case for a condensed phase system, will also smear out the quantum beats. Accordingly, our results concerning the amplitudes of the quantum beats and their modulation, constitute an upper limit.

Nonadiabatic dynamics in the condensed phase, e.g., ET transfer of type (1.1), is amenable to the theoretical description in terms of nonradiative decay into a Franck–Condon quasicontinuum. Our theoretical and numerical analysis of the temporal coherence effects in nonadiabatic dynamics in the Franck–Condon system can be confronted with the experimental results of Hochstrasser *et al.*[34] for ET in Mulliken-type charge transfer complexes,[35] Eq. (1.1). Our theoretical analysis predicts the following.

(a) Low amplitude of coherent temporal modulation. The appearance of quantum beats in the temporal decay $P(t)$ of the reactants, Eq. (6.3), and in the buildup $P_\alpha(t)$, Eq. (2.8), of the products is characterized by a modest modulation with $\xi$ being in the range of a few percent. This feature reflects the characteristics of nonradiative decay probabilities in a Franck–Condon system. The experimental data of Hochstrasser *et al.* for the dynamics of the nonradiative decay of the doorway states of the pyrene$^+$–TCNE$^-$ complex[34(b)] give $T_p = 200$ fs for the period of the beats and $\tau = 1400-1200$ fs for the decay time. Accordingly, $N_p$, Eq. (4.1), is $N_p = 6-7$ and Eq. (4.4) predicts the maximal value of the modulation amplitudes of $|\xi^{(\eta)}| = (0.17-0.14)\,\eta$. For the reasonable value of the correlation parameter $\eta = 0.3-0.4$ (Fig. 3), $|\xi^{(\eta)}| \cong 0.05-0.06$, which concurs with the experimental results.[34(b)] We should note that we did not consider effects of static inhomogeneous broadening and of additional smearing of the quantum beats due to a contribution of a large number of vibrational modes (not taken into account in our four-mode system).

(b) Dominating contributions to temporal coherence. The most pronounced temporal modulation (reflected in the largest values of $|\eta_{ss'}|$) originated from coherence between doorway states, e.g., $s,s'$, which correspond to members of a single vibrational progression with $\Delta v = 1$. Thus the period(s) $T_{p'}$ of the pronounced quantum beats is dominated by single-mode vibrational frequencies. The propensity rule

$\Delta v_j = \pm 1$ for the dominant contribution to temporal coherence is borne out in the experimental data for $P(t)$ and $P_\alpha(t)$ of charge transfer complexes[34] where the vibrational temporal coherence is determined by $|E_s - E_{s'}|$, which corresponds to the intermolecular $D^+ - A^-$ (or $D-A$) vibrational frequency of the complex.[34(b)]

## ACKNOWLEDGMENTS

This research was supported by the Deutsche Forschungsgemeinschaft (Sonderforschungsbereich 377) and by the Volkswagen Stiftung.

[1] A. H. Zewail, *Femtochemistry* (World Scientific, Singapore, 1994).
[2] *Femtosecond Chemistry*, edited by J. Manz and L. Wöste (VCH Weinheim, 1995).
[3] *Femtochemistry*, edited by M. Chergui (World Scientific, Singapore, 1996).
[4] S. Mukamel, Annu. Rev. Phys. Chem. **41**, 647 (1990).
[5] V. S. Lethokov, in Ref. 3, p. 25, and references therein.
[6] J. Jortner, in Ref. 3, p. 15, and references therein.
[7] (a) R. M. Bowman, M. Dantus, and A. H. Zewail, Chem. Phys. Lett. **161**, 297 (1989); (b) M. Dantus, R. M. Bowman, and A. H. Zewail, Nature **343**, 737 (1990); (c) M. Bruebele, G. Roberts, M. Dantus, R. M. Bowman, and A. H. Zewail, Chem. Phys. Lett. **166**, 459 (1990); (d) J. J. Gerdy, M. Dantus, R. M. Bowman, and A. H. Zewail, *ibid*. **171**, 1 (1990); (e) M. Gruebele and A. H. Zewail, J. Chem. Phys. **98**, 883 (1993); (f) R. M. Bowman, M. Dantus, and A. H. Zewail, Chem. Phys. Lett. **156**, 131 (1989); (g) M. Dantus, R. M. Bowman, M. Gruebele, and A. H. Zewail, J. Chem. Phys. **91**, 7437 (1989); (h) S. Pedersen, T. Baumert, and A. H. Zewail, J. Phys. Chem. **97**, 12460 (1993).
[8] (a) T. Baumert, M. Grosser, R. Thalweiser, and G. Gerber, Phys. Rev. Lett. **67**, 3753 (1991); (b) T. Baumert, B. Buhler, M. Grosser, R. Thalweiser, V. Weiss, E. Wiedenmann, and G. Gerber, J. Phys. Chem. **95**, 8103 (1991); (c) T. Baumert, V. Engel, C. Rottgermann, W. T. Strunz, and G. Gerber, Chem. Phys. Lett. **191**, 639 (1992); (d) T. Baumert, V. Engel, C. Meier, and G. Gerber, *ibid*. **200**, 488 (1992).
[9] (a) N. F. Scherer, A. J. Ruggiero, M. Du, and G. R. Fleming, J. Chem. Phys. **93**, 856 (1990); (b) N. F. Scherer *et al.*, *ibid*. **95**, 1487 (1991); (b) N. F. Scherer, A. Matro, L. D. Ziegler, M. Du, R. J. Carlson, J. A. Cina, and G. R. Fleming *ibid*. **96**, 4180 (1992).
[10] T. J. Dunn, J. N. Sweeter, I. A. Walmsley, and C. Radzewicz, Phys. Rev. Lett. **70**, 3388 (1993).
[11] V. Blanchet, M. A. Bouchene, O. Cabrol, and B. Girard, Chem. Phys. Lett. **233**, 491 (1995).
[12] (a) E. D. Potter, Q. Liu, and A. H. Zewail, Chem. Phys. Lett. **200**, 605 (1992); (b) Q. Lui, J.-K. Wang, and A. H. Zewail, Nature **364**, 427 (1993); (c) J.-K. Wang, Q. Liu, and A. H. Zewail, J. Phys. Chem. **99**, 11309 (1995); (d) Q. Lui, J.-K. Wang, and A. H. Zewail, *ibid*. **99**, 11321 (1995).
[13] (a) C. Lienau, J. C. Williamson, and A. H. Zewail, Chem. Phys. Lett. **213**, 289 (1993); (b) C. Lienau and A. H. Zewail, *ibid*. **222**, 224 (1994); (c) C. Lienau and A. H. Zewail, J. Chim. Phys. **92**, 566 (1995).
[14] (a) J. M. Papanikolas, J. R. Gord, N. E. Levinger, D. Ray, V. Vorsa, and W. C. Lineberger, J. Phys. Chem. **95**, 8028 (1991); (b) J. M. Papanikolas, V. Vorsa, M. E. Nadal, P. J. Campagnola, J. R. Gord, and W. C. Lineberger, J. Chem. Phys. **97**, 7002 (1992); (c) J. M. Papanikolas, V. Vorsa, M. E. Nadal, P. J. Campagnola, H. K. Buchenau, and W. C. Lineberger, *ibid*. **99**, 8733 (1993).
[15] J. M. Papanikolas, P. E. Maslen, and R. Parson, J. Chem. Phys. **102**, 2452 (1995).
[16] (a) U. Banin, A. Waldman, and S. Ruhman, J. Chem. Phys. **96**, 2416 (1992); (b) U. Banin and S. Ruhman, *ibid*. **98**, 4391 (1993); (c) I. Benjamin, U. Banin, and S. Ruhman, *ibid*. **98**, 8337 (1993).
[17] B. J. Schwartz, J. C. King, J. Z. Zhang, and C. B. Harris, Chem. Phys. Lett. **203**, 503 (1993).
[18] (a) R. Zadoyan, Z. Li, P. Ashjian, C. C. Martens, and V. A. Apkarian, *Ultrafast Phenomena* (Springer, Berlin, 1994), Vol. 7; (b) R. Zadoyan, Z. Li, P. Ashjian, C. C. Martens, and V. A. Apkarian, Chem. Phys. Lett. **218**, 504 (1994); (c) R. Zadoyan, Z. Li, C. C. Martens, and V. A. Apkarian, in *Laser Techniques for State-Selected and State-to-State Chemistry II*, edited by J. W. Hepburn [Proc. SPIE **2124**, 233 (1994)]; (d) R. Zadoyan, Z. Li, C. C. Martens, and V. A. Apkarian, J. Chem. Phys. **101**, 6648 (1994); (e) Z. Li, R. Zadoyan, V. A. Apkarian, and C. C. Martens, J. Phys. Chem. **99**, 7453 (1995).
[19] N. Pugliano, D. K. Palit, A. Z. Szarka, and R. M. Hochstrasser, J. Chem. Phys. **99**, 7273 (1993).
[20] A. Z. Szarka, N. Pugliano, D. K. Palit, and R. M. Hochstrasser, Chem. Phys. Lett. **40**, 25 (1995).
[21] (a) W. B. Bosma, Y. J. Yan, and S. Mukamel, J. Chem. Phys. **93**, 3863 (1990); (b) Y. J. Yan and S. Mukamel, *ibid*. **94**, 997 (1991); (c) S. Mukamel and Y. Yan, J. Phys. Chem. **95**, 1015 (1991); (d) L. E. Fried and S. Mukamel, J. Chem. Phys. **93**, 3063 (1990).
[22] (a) J. M. Jean, R. A. Friesner, and G. R. Fleming, J. Chem. Phys. **96**, 5827 (1992); (b) J. M. Jean and G. R. Fleming, *ibid*. **103**, 2092 (1995); (c) J. M. Jean, G. R. Fleming, and R. A. Friesner, Ber. Bunsenges. Phys. Chem. **95**, 253 (1991).
[23] (a) J. N. Onuchic and P. G. Wolynes, J. Phys. Chem. **92**, 6495 (1988); (b) S. S. Skourtis, A. J. R. de Silvia, W. Bialek, and J. N. Onuchic, *ibid*. **96**, 8034 (1992).
[24] F. Zhu, C. Galli, and R. M. Hochstrasser, J. Chem. Phys. **98**, 1042 (1993).
[25] M. Ben-Nun and R. D. Levine, Chem. Phys. Lett. **203**, 450 (1993).
[26] M. Ben-Nun, R. D. Levine, and G. R. Fleming, J. Chem. Phys. **105**, 3035 (1996).
[27] (a) M. H. Vo, J.-C. Lanbry, S. J. Robles, D. C. Youvan, J. Breton, and J.-L. Martin, Proc. Natl. Acad. Sci. USA **88**, 8855 (1991); (b) M. H. Vos, F. Rappaport, J.-C. Lambry, J. Breton, and J.-L. Martin, Nature **365**, 320 (1995); (c) M. H. Vos, M. R. Jones, C. N. Hunter, J. Breton, J.-C. Lambry, and J.-L. Martin, Biochemistry **33**, 6750 (1994); (d) R. J. Stanley *et al.*, J. Phys. Chem. **99**, 859 (1995).
[28] (a) L. Zhu, J. T. Sage, and P. M. Champion, Science **266**, 629 (1994); (b) W. D. Tian, J. T. Sage, P. M. Champion, E. Chien, and S. G. Sligar, Biochemistry **35**, 3487 (1996).
[29] (a) S. L. Dexheimer, R. A. Mathies, Q. Wang, L. A. Peteanu, W. T. Pollard, and C. V. Shank, Chem. Phys. Lett. **188**, 61 (1992); (b) W. T. Pollard, S. L. Dexheimer, Q. Wang, L. A. Peteanu, R. A. Mathies, and C. V. Shank, *ibid*. **96**, 6147 (1992); (c) L. A. Peteanu, R. W. Schoenlein, Q. Wang, R. A. Mathies, and C. V. Shank, Proc. Natl. Acad. USA **90**, 11762 (1993); (d) Q. Wang, R. W. Schoenlein, L. A. Peteanu, R. A. Mathies, and C. V. Shank, Science **L60**, 422 (1992).
[30] (a) M. Chachisvilis, T. Pullerits, M. R. Jones, C. N. Hunter, and V. Sundström, Chem. Phys. Lett. **224**, 345 (1994); (b) M. Chachisvilis and V. Sundström, *ibid*. (in press); (c) T. Pullerits and V. Sundström, Acct. Chem. Res. (in press).
[31] S. E. Brandforth, R. Jimenez, F. Van Mourik, R. Van Grondelle, and G. R. Fleming, J. Phys. Chem. **99**, 16179 (1995).
[32] (a) R. S. Berry and J. Jortner, J. Chem. Phys. **48**, 2757 (1968); (b) M. Bixon, Y. Dothan, and J. Jortner, Mol. Phys. **17**, 109 (1969).
[33] (a) N. F. Scherer, L. D. Ziegler, and G. R. Fleming, J. Chem. Phys. **96**, 5544 (1992); (b) N. F. Scherer, D. M. Jonas, and G. R. Fleming, *ibid*. **99**, 153 (1993).
[34] (a) K. Wynne, C. Galli, and R. M. Hochstrasser, J. Chem. Phys. **100**, 4797 (1994); (b) K. Wynne, G. D. Reid, and R. M. Hochstrasser, *ibid*. **105**, 2287 (1996).
[35] R. S. Mulliken and W. B. Parson, *Molecular Complexes* (Wiley, New York, 1969).
[36] J. Tang and S. H. Lin, Chem. Phys. Lett. **254**, 6 (1996).
[37] Z. Li, J. Y. Fung, and C. C. Martens, J. Chem. Phys. **104**, 6919 (1996).
[38] (a) U. Banin, R. Kosloff, and S. Ruhman, Isr. J. Chem. **33**, 141 (1993); (b) U. Banin, A. Bartana, and R. Kosloff, J. Chem. Phys. **101**, 8461 (1994); (c) U. Banin, R. Kosloff, and S. Ruhman, Chem. Phys. **183**, 289 (1994).
[39] A. G. Redfield, Adv. Magn. Reson. **1**, 1 (1965).
[40] (a) S. Mukamel and J. Jortner, in *The World of Quantum Chemistry*, edited by R. Daudel and B. Pullman, Proceedings of the First International Congress of Quantum Chemistry, Menton, France, 1973 (Reidel Dordrecht, 1974), pp. 145–209; (b) S. Mukamel and J. Jortner, in *MTP International Review of Science*, edited by A. D. Buckingham and C. A. Coulson (Butterworth, London, 1976), Vol. 13, p. 327; (c) S. Mukamel and J. Jortner, in *Excited States*, edited by E. C. Lim (Academic, New York, 1977), Vol. III, pp. 57–107.
[41] M. Bixon and J. Jortner, J. Chem. Phys. **48**, 715 (1968).
[42] E. P. Wigner, Ann. Math. Lpz. **62**, 548 (1955); **67**, 325 (1958).
[43] R. J. Elliot, J. A. Krumhansl, and A. Leath, Rev. Mod. Phys. **46**, 405 (1974).

[44] (a) W. M. Gelbart, S. A. Rice, and K. F. Freed, J. Chem. Phys. **57**, 4679 (1972); (b) W. M. Gelbart, D. F. Heller, and M. L. Elert, Chem. Phys. **7**, 116 (1975); (c) K. G. Kay, J. Chem. Phys. **61**, 5205 (1974); (d) J. Kommandeur and J. Jortner, Chem. Phys. **28**, 273 (1978); (e) A. Nitzan and J. Jortner, J. Chem. Phys. **71**, 3524 (1979).

[45] (a) J. Jortner, Adv. Laser Spectrosc. **113**, 88 (1977); (b) B. Carmeli and A. Nitzan, Chem. Phys. Lett. **58**, 310 (1978); (c) I. Schek and J. Jortner, J. Chem. Phys. **70**, 3016 (1979); (d) B. Carmeli and A. Nitzan, *ibid*. **72**, 2054, 2080 (1980); (e) B. Carmeli, I. Schek, A. Nitzan, and J. Jortner, *ibid*. **72**, 1928 (1980).

[46] (a) F. H. Mies and M. Kraus, J. Chem. Phys. **45**, 4453 (1965); (b) S. A. Rice, I. J. McLaughlin, and J. Jortner, *ibid*. **49**, 2756 (1968); (c) M. Bixon and J. Jortner, *Dynamics in the Franck–Condon Quasicontinuum* (to be published).

[47] M. Bixon and J. Jortner, Chem. Phys. **176**, 467 (1993).